Journal of Materials Chemistry A

High Throughput Finding Li Ion Diffusion Pathway in Typical Solid State Electrolytes and Electrode Materials by BV-Ewald Method

Journal:	*Journal of Materials Chemistry A*
Manuscript ID	TA-ART-09-2018-009345.R1
Article Type:	Paper
Date Submitted by the Author:	05-Dec-2018
Complete List of Authors:	Chen, Dajun; Peking University, School of Advanced Materials Jie, Jianshu; Peking University Shenzhen Graduate School, School of Advance Materials Weng, Mouyi ; School of Advanced Materials, Shenzhen Graduate School, Peking University Li, Shucheng; Peking University, School of Advanced Materials Chen, Dong; Peking University Shenzhen Graduate School, School of Advance Materials Pan, Feng; Peking University, School of Advanced Materials Wang, Lin-Wang; Lawrence Berkeley National Laboratory,

Journal of Materials Chemistry A

ARTICLE

High Throughput Finding Li Ion Diffusion Pathway in Typical Solid State Electrolytes and Electrode Materials by BV-Ewald Method

Received 00th January 20xx,
Accepted 00th January 20xx

DOI: 10.1039/x0xx00000x

www.rsc.org/

Dajun Chen[a], Jianshu Jie[a], Mouyi Weng[a], Shucheng, Li[a], Dong Chen[a], Feng Pan*[a] and Lin-Wang Wang*[b]

Viewing possible Li-ion migration pathways in solid state electrolytes and electrode materials is an important prerequisite for the discovery of all-solid-state batteries materials. For high throughput material screening, it is important to have a fast method to find the possible Li-ion pathways. In this work, by combining traditional bond valence (BV) method with Ewald summation method, a new BV-Ewald method is developed to calculate the Li ion diffusion map. Advantage of the new method is to improve the traditional BV method by taking into account the cation-cation Coulomb repulsion. By adjusting isosurface value, the BV-Ewald method can reveal the Li pathway of several well-studied electrolytes (e.g. Li_3OCl, $LiTi_2(PO_4)_3$, α-Li_3N and β-Li_3N) and cathode materials (e.g. $LiFePO_4$, $LiMn_2O_4$) quite well to match with the experimental and ab initio calculation results. Furthermore, this new high throughput method is used for fast predicting Li-ion 1D, 2D and 3D-pathways of (anti)perovskite，NASICON，LISICON，Garnet，Li-nitride，Li-hydride，Li-Halide and Argyrodite types of crystals with 34 different known electrode and electrolytes as representors. Hence, the new BV-Ewald method will help for fast discovering potential solid electrolyte materials.

1. Introduction

Lithium (ion) batteries (LIBs) have been widely used in our lives such as mobile phones, notebook computers[1] and hybrid electric vehicles[2,3] due to their large specific capacity, long storage and cycle life, and environmental friendliness. However, current LIBs mainly use liquid electrolytes which are easy to cause leakage and safety problems[4]. All-solid-state batteries consist of solid electrodes and solid electrolytes[5] are promising next-generation LIBs. One of the primary conditions for both inorganic solid electrodes and solid electrolytes is the high lithium ionic conductivity and the connected lithium ion pathway. Experimentally, lithium ion channels can be measured directly by neutron diffraction[6,7]. Theoretically, the Li ion migration pathway can be acquired by the first-principles simulations[8–11]. These can be the direct ab initio molecular dynamics (MD) simulations, or barrier height nudge elastic band (NEB) calculations. However, such calculations can be very expensive (the MD simulation), or require prior knowledge for what are the transition paths (NEB). Because of these difficulties, such ab initio methods are not suitable for high throughput screening of possible solid electrolyte or electrode materials. Some computationally fast method will be extremely useful, either for high throughput screening, or to provide initial insights for more in-depth ab initio studies (e.g. using NEB). There are several methods for such purpose. One is the bond valence (BV) method[10–14], the others are geometry based methods like Voroni-Dirichlet partition (VDP)[15], Colony surface[16], and Procrystal analysis[17]. The geometry based methods rely solely on the crystal structure and bonding topology, not taking into account of any actual potential energies. The BV model has been widely used in crystallography to determining the position occupied by atoms in the crystal structure [18] , as well as being used to visualize the Li pathway[12,17]. However, when BV is used to visualize the Li pathway, it only takes into account the effects of surrounding anode atoms, and ignores the electrostatic repulsion to the cations[18]. This can lead to some erroneous results, e.g. the Li concentration on top of other cation atoms. It is this aspect of the BV method we aim to improve in the current paper.

We combine the BV theory and Ewald summation which is used to calculate the coulomb repulsive between Li ion and other cations to improve the original BV method. Only the Coulomb interactions with cation atoms are included since the interactions with anion atoms have already been described by the BV model. We calculated several materials and compare the results with ab initio molecular dynamic simulations and found they are in good agreements. By further analyzing the results, we found that the new BV-Ewald method can improve the original BV method in many structures, such as Li_3N and $LiFePO_4$. In $LiFePO_4$, the original BV model yield Li density on top of the Fe atom, a clearly unphysical result. In Li_3N the BV yield different Li diffusion path compared to ab initio results.

[a] School of Advanced Materials, Peking University, Shenzhen Graduate School, Shenzhen 518055, People's Republic of China. E-mail: panfeng@pkusz.edu.cn
[b] Materials Science Division, Lawrence Berkeley National Laboratory, Berkeley, California 94720, United States. *E-mail: lwwang@lbl.gov
†Electronic Supplementary Information (ESI) available: See DOI: 10.1039/x0xx00000x

Both these errors have been corrected by the BV-Ewald method. Finally, we have calculated the Li pathways of 34 typical cathode/anode electrodes and solid electrolytes materials, and determined the dimensionalities of their transition paths, whether it is 1D, 2D or 3D path. Not only can we get Li diffusion pathway, but also other ionic diffusion pathway such as Na in sodium ion batteries. There are already many researches in screening sodium-based layered materials for sodium ion batteries[19–21]. Our method can also be used in this area to further screen sodium ion battery materials.

2. Methodology

The original BV method was put forward by Ian David Brown to describe the relationship between bonding length and charge transfer: the shorter the bond length, the larger the charge transfer between cation and anions. [18] It includes four heuristic principles: principle of maximum symmetry, electroneutrality principle, principle of local charge neutrality and equal valence principle [18]. The valence charge transfer based on the cation-anion bond length is described by:

$$S_{A-x} = \exp[\frac{R_0 - R_{A-X}}{b}] \quad (1)$$

Then the valence charge on atom A is described as:

$$\mathrm{V(A)} = \sum_{X} S_{A-x} \quad (2)$$

In above, A is the cation and X is the anion, $R_{A\text{-}X}$ is their distance. R_0 and b are empirical parameters. S_{A-x} is bond valence of A contributed by the X in the given position and $\mathrm{V(A)}$ is the BV sum that should be close to the ideal chemical valence $V_{ideal}(\mathrm{A})$. Thus, the deviation between V(A) and $V_{ideal}(\mathrm{A})$ determines the energy of this structure. BV theory does not require a specific distinction between covalent and ionic types of bonding. Cation and anion here are defined by their electronegativity and are equivalent to Lewis acids and bases. [19] In practice, we can assume that the central cation A only interacts with X within a cutoff distance of about 10 Å. When applying the BV for Li pathway visualization, one calculates the V(Li) for a hypothetical Li atom at a given position x, and assume $V_{ideal}(\mathrm{Li}) = 1$. Then the spatial function $|\triangle \mathrm{V(x)}| = |\mathrm{V(Li)} - V_{ideal}(\mathrm{Li})|$ can be used to visualize the Li charge density. Smaller this value, larger should be the Li charge density. This BV method has been extensively used in searching for the Li path. For example, Adams' et.al [22-26] developed a program based on BV to obtain the three-dimensional atomic valence map which could be regarded as the "ion diffusion channel". They have also related their BV calculated results to energy manifold (similar to the transition barrier) [25,26]. Due to the low computational cost of this method, the group has completed the calculation and screening of lithium ion diffusion channels in all alkaline earth metal ion materials in the Inorganic Crystal Structure Database (ICSD)[27]. In another example, Chen et.al[28] has combined the advantages of BV and DFT to carry out a high-throughput design and optimization of fast lithium ion conductors using β-Li_3PS_4 as an example.

However, the BV method only considers the Li interaction with anions, completely ignoring the existence and the position of cations. It is easy to imagine this can lead to errors. Indeed, the diffusion pathways provided by the BV theory can often be different from those obtained by first-principles molecular dynamics simulation[29,30]. For example, in the $LiFePO_4$, the BV pathway will include Fe atom and in the Li_3N, the BV pathway is completely wrong. We will discuss these examples later in the paper.

Here, we use Ewald summation between Li atom and the cathode atoms to overcome this shortcoming of the BV method. We only include the Li-cation interaction since the Li-anion interaction has already been taken into account by the BV method. What calculated is essentially the Li-cation Coulomb interaction within a uniform negative charge background to compensation the total positive charge of the cations. To calculate such Coulomb interaction, the Ewald summation is used in both real space and reciprocal space[31]. The Ewald summation divides the long range Coulomb interaction into two parts: a short-range contribution which is calculated in real space and a long-range contribution which is calculated using a Fourier transformation. By setting the G=0 component in the Fourier space to be zero, the uniform negative charge back ground can be taken into account. Although the Ewald summation equation is very standard, we include it here for completeness:

$$U_{Ewald} = U_{real} + U_{reciprocal} + U_{correction} \quad (3)$$

where

$$U_{real} = \frac{1}{4\Pi\varepsilon_0} \cdot \frac{1}{2} \sum_{\vec{n}}^{*} \sum_{i=1}^{N} \sum_{j=1}^{N} q_i q_j \frac{erfc(\alpha|\vec{x}_{ij} + \vec{n}|)}{|\vec{x}_{ij} + \vec{n}|} \quad (4)$$

$$U_{reciprocal} = \frac{1}{\varepsilon_0 V} \cdot \frac{1}{2} \sum_{\vec{k}\neq\mathbf{0}} \frac{1}{\vec{k}^2} e^{-\frac{\vec{k}^2}{4\alpha}} \left[\left| \sum_{i=1}^{N} q_i \cos(\vec{k} \cdot \vec{x}) \right|^2 + \left| \sum_{i=1}^{N} q_i \sin(\vec{k} \cdot \vec{x}) \right|^2 \right] \quad (5)$$

and $U_{correction}$ is a constant depending on the parameter α. The converged results should not depend on the choice of α.

The Ewald Coulomb repulsive potentials (U_{Ewald}) are calculated on a regular 3D real space grids for the Li position. In such a calculation, we imagine a testing Li atoms walking through the whole 3D space. One issue arrives: how to deal with the interaction of this testing Li atom and the real Li atom existing in the crystal (e.g., in its ground state position). Since we are using this imaginary testing Li atom to represent all the Li atoms in the system, the repulsive interaction between this testing Li atom to a nearby ground state Li atom is an erroneous interaction between the Li atom itself (since the testing Li atom is representing the nearby ground state Li atom for which it interacts with). We thus need to remove this "self-interaction". However, we should keep the interaction with the Li atom far away since they are the "other" Li atoms. We thus have:

$$U_e = U_{Ewald} - U_{Li} \quad (6)$$

and the following formula is used to calculate U_{Li} for interaction with nearby Li atoms:

$$U_{Li} = \frac{1}{4\pi\varepsilon_0} \cdot \sum_{R_{cut}} \frac{q_{Li}^2}{R} e^{-\beta \cdot R^2} \quad (7)$$

R is the distance between grid point (the position of the test Li atom) and the Li ion around that point, and β is a parameter to control the range of this exclusion. We have chosen β equals the one over square of 0.38 Å, half of the lithium ion radius.
Now, we have two quantities: one is the BV valence V(Li) of Eq(2), another the U_e of Eq(6). Our next task is to combine these two quantities into a single value to represent the Li concentration on the 3D grid. One option is to add them together as two energy components. Another option is to multiply them together as two factors. Adding them together require careful weighting in order to deal with their possible compensations. Tests show it is difficult to yield a reliable result. On the other hand, by multiplying them, we can require the system to satisfy two conditions: the bond valence to be close to 1, and the U_e to be very negative (which is always negative due to the negative back ground compensation, thus we require $|U_e|$ to be large). After some tests, we arrived at the following empirical expression:

$$E(BV - Ewald) = \frac{1}{|V(Li) - 1|^{10} + 1} \cdot |U_e| \quad (8)$$

Larger this value E(BV-Ewald), higher probability of Li. To visualize the Li path, we thus use an isosurface value E_{iso}. For a given positon x in the real space 3D grid, if E(BV-Ewald) > E_{iso}, the lithium will occupy that point. This can thus give us the Li diffusion path. However, the E_{iso} for different systems can be different. In practice, one decreases the E_{iso} from large to small, until the isosurface connects the Li path from one side of the crystal to the other side. In the following, the Li path will be represented by the isosurface of E_{iso} plotted with the VESTA visualization package[32]. The computation time for most structure is several minutes which improves the efficiency greatly compared to first-principles molecular dynamics simulation. Such a code can thus be used for high throughput screening of solid electrolyte materials. The BV code is written in python and the Ewald code is written by Fortran. The crystal structures are taken from MP database[33] and Material Go database [34].

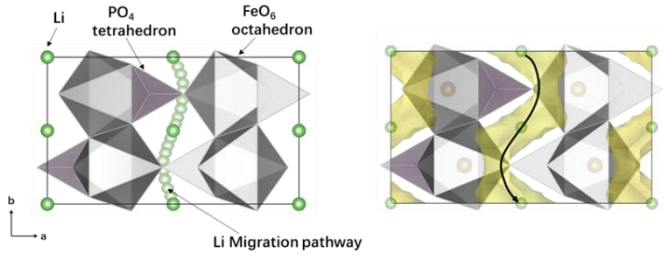

Figure 1 Li migration pathway of $LiFePO_4$. Left: schematic view of the ab initio molecular simulation Li ion diffusion channel（Ref. [26]); right: BV-Ewald isosurface of Li ion diffusion pathway with E_{iso} =42.5. The black arrowed line in the right panel is a replot of the path from the left panel. The PO_4 tetrahedron is light purple and the silver-gray polyhedron is FeO_6 octahedron

3. Result and Discussion

In order to test the accuracy of the BV-Ewald method, we have predicted the diffusion pathways of several well-studied materials. The first material is $LiFePO_4$ which has attracted a lot of interest and has already been used as cathode material of Li-ion battery commercially due to its environment-friendliness and low cost of Fe element [35]. $LiFePO_4$ is an olivine-structured orthophosphate as shown in **Figure 1**. The left picture shows schematically the Li ion migration pathway calculated by ab initio molecular dynamic [33]. The right picture shows the BV-Ewald result. The yellow part is the isosurface representing the Li clouds (populations) calculated by the BV-Ewald method with E_{iso}=42.5. We can see that the Li ion migration pathway is along with the b axis which is in good agreement with the ab initio calculation results [35,36]

It is helpful to understand the Li transition path in $LiFePO_4$, and why the BV-Ewald model can capture such transition path. There are three possible Li paths in $LiFePO_4$, as shown in **Figure 2**. The path 1 along the b axis direction is clear from the PO_4 tetrahedron and the FeO_6 octahedron and there is no barrier when Li ion migrates along this path. However, in

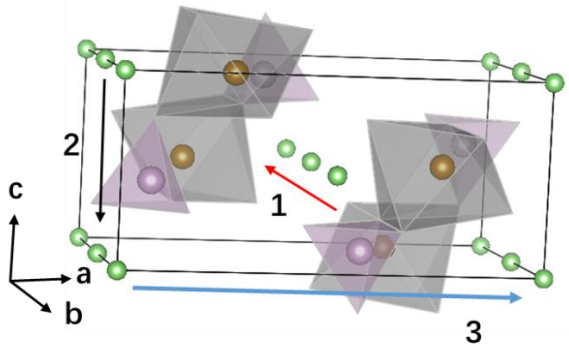

Figure 2 Structure of LiFePO4.The Li atom is green; the Fe atom is golden; the P atom is purple; the O atom is not shown.

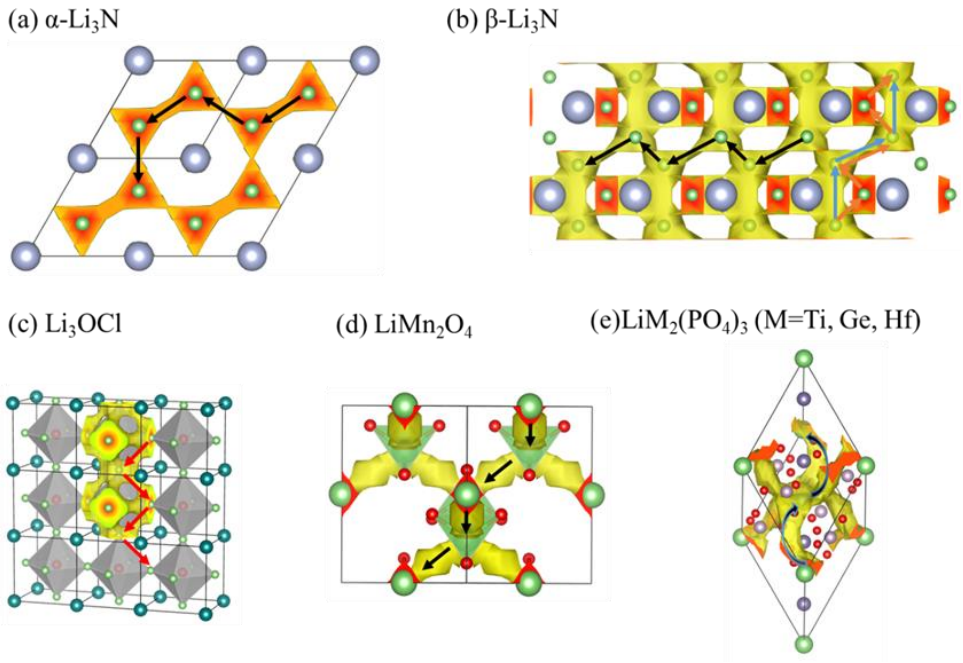

Figure 3 Comparison between ab initial path (arrowed lines) and BV-Ewald path (yellow isosurface) of Li diffusion pathways: (a) Li migration pathway of α-Li_3N. First-principles calculations of Li ion diffusion channel[9] and BV-Ewald result of Li ion diffusion pathway when E_{iso} =3.6. (b) Li migration pathway of β-Li_3N. First-principles calculations of Li ion diffusion channel[9] and BV-Ewald result of Li ion diffusion pathway when E_{iso} =6. (c) Li migration pathway of Li_3OCl. The arrow shows the migration pathway calculated by ab initio calculations and the Gibbs energy down the route goes from ca. 0.290 eV at 0 K to ca. 0.245 eV before the melting point (550 K)[37] and the yellow part is BV-Ewald result of Li ion diffusion pathway when E_{iso} =2.6. (d) Li migration pathway of $LiMn_2O_4$. First-principles calculations of Li ion diffusion channel[35] and the BV-Ewald result of Li ion diffusion pathway when E_{iso} =70. (e) Li migration pathway of $LiM_2(PO_4)_3$ (M=Ti, Ge, Hf)[39]. Negative nuclear density maps after MEM reconstruction and the BV-Ewald result of Li ion diffusion pathway when E_{iso} =139.5

path 2 and 3, Li ion has to go through the side of PO_4 tetrahedron and FeO_6 octahedron that will influence the transfer of Li ion. What's more, the distance from one Li ion location to another location along path1 is shortest in path 1 (which is about 3.04 Å), compared to that of path2 and path3 (which are 4.75 Å and 10.45 Å respectively). So the most possible Li migration pathway is path1 down the b direction. Fisher[35] has calculated the Li ion migration energy of $LiFePO_4$. The energy barrier pathway of path 1 is 0.55 eV; the barrier of the path2 is 2.89 eV and the barrier of the path3 is 3.36eV. Our BV-Ewald method calculates the Coulomb repulsive interaction between Fe/P and Li on every grid, the energy along the path1 is the smallest due to its relative long distance from the cation. On the other hand, the path 2 and 3 will encounter the Fe/P cations in some short distance along the path, thus increase their energies.

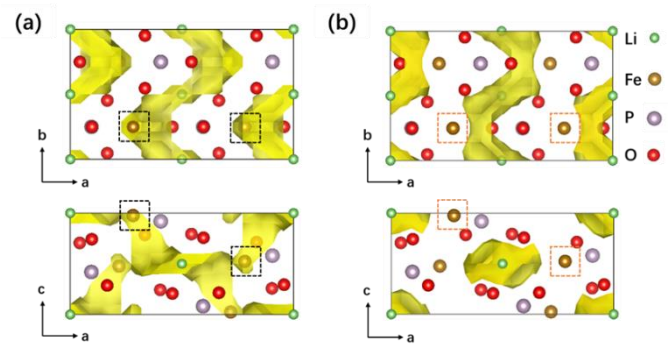

Figure 4 (a) Li diffusion map of $LiFePO_4$ calculated by BV method; (b) Li diffusion map calculated by BV-Ewald method. The green ball is Li atom, the brownness ball is Fe atom, the light purple ball is phosphorus atom and the red ball is oxygen atom

We have also calculated several other well-known cathode and solid electolyte materials such as $LiMn_2O_4$, Li_3OCl, $LiM_2(PO_4)_3$ (M=Ti, Ge, Hf), α-Li_3N and β-Li_3N with their BV-Ewald Li diffusion path shown in Figure3. These few systems are selected due to the existence of ab initio molecular dynamics (MD) simulations of their Li diffusion paths. The results of these ab initio MD simulations are summarized for their Li diffusion paths as represented by the arrowed lines in **Figure 3**. As can be seen in Figure 3, the BV-Ewald reproduced these ab initio paths perfectly. This shows a major success of the BV-Ewald method.

In the following, we compare the BV-Ewald result with the BV result, just to see in what cases, the BV-Ewald can improve the BV result. We use again $LiFePO_4$ as our first example. As illustrated in **Figure 4**, the left part (**a**) is the Li ion diffusion map that is calculated by BV method (with isosurface on |V(Li)-1|<0.1) and the right part (**b**) is BV-Ewald calculated results. We find that both methods show the Li migration pathway along the b axis. However, there is a crucial difference. As circled in the black square in Figure 4a, the BV Li map includes Fe atoms inside its isosurface no matter what isosurface value is chosen. This is obviously not correct, since it implies the Li will be on position of the Fe atoms. This is a result of ignoring the Li-cation repulsion. On the contrary, the BV-Ewald Li map does not contain the Fe atom as shown Figure 4b.

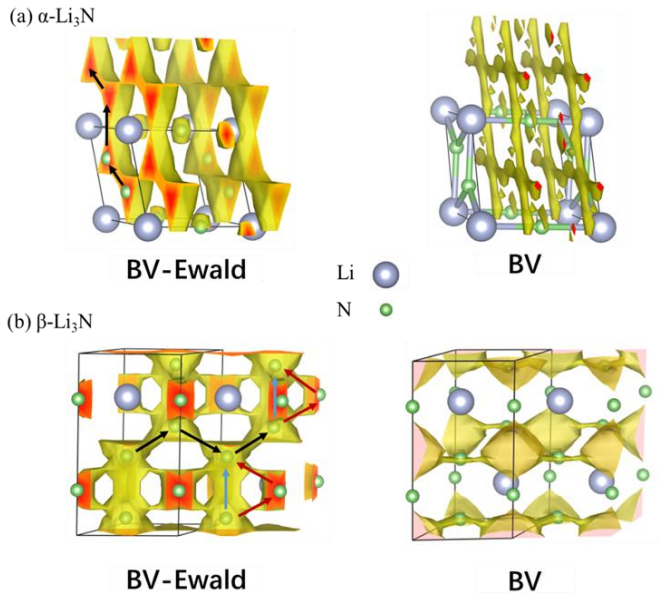

Figure 5 (a) Li diffusion map of α-Li_3N; (b) Li diffusion map of β-Li_3N. The green ball is Li and grey ball is N. The arrows describe the Li ion migration pathway by using First-principles calculations

In the above example of $LiFePO_4$, although the isosurface between BV and BV-Ewald are different around Fe position, the Li diffusion paths of them are roughly the same. However, this is not always the case for other systems. We find that the BV and BV-Ewald Li ion diffusion pathways in Li_3N are completely different. In the **Figure 5,** the left picture is the result of BV-Ewald and the right picture is the result of BV theory. The arrows describe the Li ion migration pathway based on first-principles calculations[9]. We can see the BV-Ewald results of α-Li_3N and β-Li_3N are in good agreement with the arrows, but the BV results are completely different. In α-Li_3N, Li ion is more likely to migrate in a shorter distance in the plane including both N and Li. In β-Li_3N, Li migration pathways also prefer the shorter Li hopping distance channel and there are three possible pathways because their hopping distances are similar. The main difference between BV and BV-Ewald method is at the Li-Li interaction. For example, for the α-Li_3N, in the BV method, the pathways are in the plane of the pure Li atoms. On the other hand, due to the Li-Li repulsion, in the BV-Ewald method, the pathways have been pushed into the Li-N plane, which agrees with the first principle results. This example shows that the Li-cation interaction as included in the BV-Ewald method can play an important role in determine the true Li diffusion path in the material. Thus, BV-Ewald method can be used for high throughput finding Li-pathway in different types of cathode and solid-electrolyte materials.

Taking the advantage of the fast calculation speed, we have calculated 34 existed typical solid state electrolytes and electrode materials. Although all these materials are known, but not all their Li diffusion paths have been studied theoretically. We like to identify the dimensionality of their Li diffusion path. This is defined as the connection dimension for the highest isosurface value where at least one direction has been connected. If only one direction has been connected at this isosurface value, the system will be called 1D. In some system, due to symmetry or other reasons, at this isosurface value, or a value slightly larger (+0.5) two directions, or all three directions will be connected, then their dimensionality will be 2D and 3D respectively. For example, the 1D pathway down the b direction in $LiFePO_4$ firstly appears with decreasing isosurface value, so its pathway is 1D. On the other hand, for $LiMn_2O_4$, 3 equivalent paths along three directions are all connected for a given isosurface value, so its dimensionality is 3D. The Table 1 and Table 2 show the crystallographic details and proposed dimensionality of Li ion diffusion pathway for electrode materials and electrolyte materials respectively. The Li diffusion isosurfaces of these 34 crystals are all shown in Figure S1.

Finally, it should be noted that in this paper, we have mainly focused on the visualization of the Li ion diffusion path. An equally important task is to estimate the diffusion barrier height. Turns out that is a much more challenging task. In order to yield accurate barrier height, real energy estimation, instead of merit functions like Eq.(8) needs to be used. Tests show that it is difficult to use Eq.(8) to estimate the barrier height. Such task needs to be worked on in the future.

Table 1 Crystallographic details and proposed dimensionality of Li ion migration pathway for electrode materials.

Compound	Space group	a(Å)	b(Å)	c(Å)	α(°)	β(°)	γ(°)	dimensionality
Electrode materials:								
$LiFePO_4$	Pnma	10.45067	6.08735	4.75196	90	90	90	1D
$LiCoO_2$	R3-m	2.8156	2.8156	14.0542	90	90	120	2D
Li_2TiO_3	C2/c	5.0996	8.85271	9.83459	90	100.2	90	3D
$LiMn_2O_4$	Fd3- m	8.4307	8.4307	8.4307	90	90	90	3D
$LiMnO_2$	Pmmn	2.86878	4.63448	5.83251	90	90	90	2D

Table 2 Crystallographic details and proposed dimensionality of Li ion migration pathway for solid-state electrolytes.

Compound	Space group	a(Å)	b(Å)	c(Å)	α(°)	β(°)	γ(°)	dimensionality

(anti)perovskite								
Li_3OCl	Pm3m	3.90834	3.90834	3.90834	90	90	90	3D
Li_2OHCl	Pm4m	3.91	3.91	3.91	90	90	90	2D
$LiLa_5Ti_8O_{24}$	Pmm2	7.85238	7.82107	7.7691	90	90	90	2D
NASICON								
$LiTi_2(PO4)_3$	R-3c	8.61194	8.61194	8.61994	60	60	60	3D
$LiGe_2(PO4)_3$	R-3c	8.4397	8.4397	8.4397	60	60	60	3D
$LiHf_2(PO4)_3$	R-3c	8.83	8.83	8.83	60	60	60	3D
LISICON								
β-Li_3PS_4	Pnma	13.18362	8.13245	6.21318	90	90	90	3D
$Li_{10}GeP_2S_{12}$	$P4_2mc$	8.78765	8.78765	12.65755	90	90	90	3D
$Li_{10}SiP_2S_{12}$	$P4_2mc$	8.78389	8.78389	12.60642	90	90	90	3D
$Li_{10}SnP_2S_{12}$	$P4_2mc$	8.85424	8.85424	12.85128	90	90	90	3D
Garnet								
$Li_7La_3Zr_2O_{12}$	$I4_1/acd$	13.23937	13.23937	12.76846	90	90	90	3D
$Li_5La_3Nb_2O_{12}$	Ia-3d	11.36758	11.36758	11.36758	109.47	109.47	109.47	3D
$Li_5La_3Ta_2O_{12}$	Ia-4d	11.35147	11.35147	11.35147	109.47	109.47	109.47	3D
Li-nitride								
α-Li_3N	P6/mmm	3.65069	3.65069	3.88863	90	90	120	2D
β-Li_3N	$P6_3/mmc$	3.56452	3.56452	6.34898	90	90	120	2D
Li_7PN_4	P4-3n	9.40238	9.40238	9.40238	90	90	90	3D
$LiPN_2$	I4-2d	4.57145	4.57145	7.28985	90	90	90	3D
$LISi_2N_3$	$Cmc2_1$	4.8144	5.33094	5.33094	119.88	90	90	1D
Li-hydride								
Li_2HN	R3m	3.6031	3.6031	9.09702	90	90	90	2D
LiH_2N	I-4	5.067	5.067	10.284	90	90	90	3D
$LiBH_4$	$P6_3mc$	4.17997	4.17997	6.71	90	90	120	2D
Li_3AlH_6	R-3	4.53	9.27	2.86	90	90	90	3D
$LIAlH_4$	$I4_1/a$	4.5776	4.5776	10.16941	90	90	90	2D
Li-Halide								
Li_2CdCl_4	Imma	7.58329	7.76592	10.59649	90	90	90	3D
Li_2MgCl_4	Imma	7.4119	7.48861	10.48336	90	90	90	3D
Li_2ZnI_4	Pnma	7.06393	8.68383	15.00896	90	90	90	2D
Argyrodite								
Li_6PS_5Br	F4-3m	10.305	10.305	10.305	90	90	90	3D
Li_6PS_5Cl	F4-3m	10.279	10.279	10.279	90	90	90	3D
Li_6PS_5I	F4-3m	10.353	10.353	10.353	90	90	90	3D

4. Conclusions

In this paper, we presented a new high throughput method for finding the Li –diffusing path of Li-ion cathode and solid-electrolyte materials by combining BV theory with the Ewald summation between Li and cation. It improves the original BV model by including the information of Li-cation repulsion. We first calculated several common solid state electrolytes and electrode materials like $LiFePO_4$ and Li_3N, and compare their Li ion diffusion pathway with first-principles results in the literature. We found that the improved BV-Ewald model yields Li diffusion path in excellent agreement with the ab initio results. On the other hand, the original BV model might yield the wrong path, or give Li clouds on top of other cathode atoms. We have also calculated 34 different known electrode and electrolytes. We provided their Li path dimensionalities, as well as the detail Li path isosurfaces which have not been studied before theoretically. The BV-Ewald model is fast to calculate, and we believe the new BV-Ewald model can be used for future high throughput simulations for new solid electrolyte discovery. It can also be used as a first screening before in-depth ab initio simulations for a given material.

Conflicts of interest

There are no conflicts to declare。

Acknowledgements

Wang is supported by the Assistant Secretary for Energy Efficiency and Renewal Energy of the U.S. Department of Energy under the Battery Materials Research (BMR) program. This work is also financially supported by National Key R&D Program of China (2016YFB0700600), and Shenzhen Science and Technology Research Grant (No.JCYJ20150729111733470 and No.JCYJ20151015162256516).S

References

1 J.M. Tarascon and M. Armand, *Mater. Sustainable Energy*, 2010,**414**, 171–179.
2 E. Karden, S. Ploumen, B. Fricke, T. Miller and K. Snyder, *J.Power Sources*, 2007, **168**, 2–11.
3 J. B. Goodenough and Y. Kim, *Chem. Mater.*, 2010, **22**, 587–603.
4 K. Xu, *Chem. Rev.*, 2004, **104**, 4303–4418.
5 K. Takada, *Acta Mater.*, 2013, **61**, 759–770.
6 M. Yashima, M. Itoh, Y. Inaguma and Y. Morii, *J. Am. Chem. Soc.*, 2005, **127**, 3491–3495.
7 J. Han, J. Zhu, Y. Li, X. Yu, S. Wang, G. Wu, H. Xie, S. C. Vogel, F. Izumi, K. Momma, Y. Kawamura, Y. Huang, J. B. Goodenough and Y. Zhao, *Chem. Commun*, 2012, **48**, 9840.
8 C. A. Geiger, E. Alekseev, B. Lazic, M. Fisch, T. Armbruster, R. Langner, M. Fechtelkord, N. Kim, T. Pettke and W. Weppner, *Inorg. Chem.*, 2011, **50**, 1089–1097.
9 W. Li, G. Wu, C. M. Araújo, R. H. Scheicher, A. Blomqvist, R. Ahuja, Z. Xiong, Y. Feng and P. Chen, *Energy Environ. Sci*., 2010, 3, 1524.
10 S. Adams and R. P. Rao, *J. Mater. Chem.*, 2012, 22, 1426-1434.
11 S. Adams and R. Prasada Rao, *J. Mater. Chem.*, 2012, **22**, 7687.
12 S. Adams, *Solid State Ionics*, 2002, **154**–**155**, 151–159.
13 S. Adams, *J. Power Sources*, 2006, **159**, 200–204.
14 V. Thangadurai, S. Adams and W. Weppner, *Chem. Mater.*, 2004, **16**, 2998–3006.
15 N. A. Anurova and V. A. Blatov, *Acta Crystallogr., Sect. B: Struct. Sci.*, 2009, **65**, 426–434.
16 G. Nuspl, T. Takeuchi, A. Weiß, H. Kageyama, K. Yoshizawa and T. Yamabe, *J. Appl. Phys.*, 1999, **86**, 5484–5491.
17 M. Ø. Filsø, M. J. Turner, G. V. Gibbs, S. Adams, M. A. Spackman and B. B. Iversen, *Chem. - Eur. J.*, 2013, **19**, 15535–15544.
18 I. D. Brown, *Chem. Rev.*, 2009, 109, 6858–6919.
19 X. Zhao, X. Zhang, D. Wu, H. Zhang, F. Ding and Z. Zhou, *J. Mater. Chem. A*, 2016, 4, 16606–16611.
20 X. Zhang, Z. Zhang, S. Yao, A. Chen, X. Zhao and Z. Zhou, *npj Comput. Mater.* , DOI:10.1038/s41524-018-0070-2.
21 Y. Zhu, X. He and Y. Mo, *J. Mater. Chem. A*, 2016, 4, 3253–3266.
22 S. Adams, *Acta Crystallogr., Sect. B: Struct. Sci.*, 2001, **57** 278-287.
23 S. Adams and J. Swenson, *Phys. Rev. Lett.*, 2000, **84**, 4144–4147.
24 S. Adams and R. P. Rao, in *Bond Valences*, eds. I. D. Brown and K. R. Poeppelmeier, Springer Berlin Heidelberg, Berlin, Heidelberg, 2014, vol. 158, pp. 129–159.
25 S. Adams and R. P. Rao, *Phys. status solidi (a)*, 2011, **208**, 1746–1753.
26 Stefan Adams* and R. Prasada Rao, *Phys. Chem. Chem. Phys.*, 2009, **11**, 3010.
27 M. Avdeev, M. Sale, S. Adams and R. P. Rao, *Solid State Ionics*, 2012, **225**, 43–46.
28 R. Xiao, H. Li and L. Chen, *Sci. Rep.*, 2015, **5**, 1–11.
29 G. Kresse and J. Hafner, *Phys. Rev. B*, 1996, **47**, 558–561.
30 G. Kresse and J. Furthmüller, *Phys. Rev. B*, 1996, **54**, 11169–11186.
31 T. Matthey, https://core.ac.uk/display/20697861, 2005
32 K. Momma and F. Izumi, *J. Appl. Crystallogr.*, 2008, **41**, 653–658.
33 A. Jain, S. P. Ong, G. Hautier, W. Chen, W. D. Richards, S. Dacek, S. Cholia, D. Gunter, D. Skinner, G. Ceder and K. A. Persson,*APL Mater.*, 2013, **1**, 011002.
34 pkusam, http://www.pkusam.com/, (accessed August 12, 2018).
35 C. A. J. Fisher, V. M. Hart Prieto and M. S. Islam, *Chem. Mater.*, 2008, **20**, 5907–5915.
36 J. Yang and J. S. Tse, *J. Phys. Chem. A*, 2011, **115**, 13045–13049.
37 R. Mouta, M. Á. B. Melo, E. M. Diniz and C. W. A. Paschoal, *Chem. Mater.*, 2014, **26**, 7137–7144.
38 N. Ishizawa, D. du Boulay, M. Hayatsu, S. Kuze, Y. Matsushima, H. Ikuta, M. Wakihara, Y. Tabira and J. R. Hester, *J. Solid State Chem.*, 2003, **174**, 167–174.
39 M. Monchak, T. Hupfer, A. Senyshyn, H. Boysen, D. Chernyshov, T. Hansen, K. G. Schell, E. C. Bucharsky, M. J. Hoffmann and H. Ehrenberg, *Inorg. Chem.*, 2016, **55**, 2941–2945.

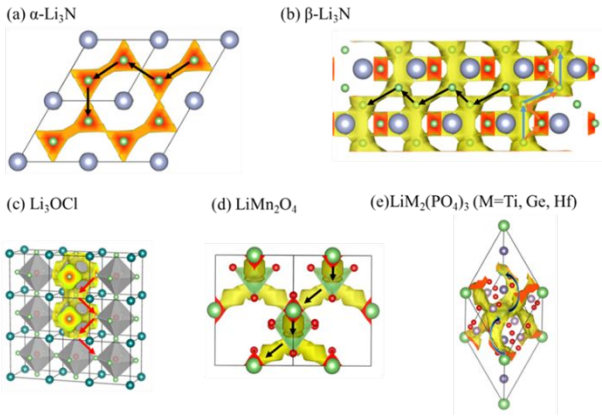

A new BV-Ewald method is developed to calculate the Li-ion diffusion pathways more quickly and correctly.